High Voltage

Research Article

IET Journals
The Institution of Engineering and Technology

Elegant procedure to estimate series capacitance of a uniform transformer winding from its measured FRA: implementable on existing FRA instruments

eISSN 2397-7264
Received on 24th September 2019
Revised 12th February 2020
Accepted on 12th March 2020
E-First on 29th May 2020
doi: 10.1049/hve.2019.0251
www.ietdl.org

Ashiq Muhammed[1], Lakshminarayana Satish[1] ✉, Udaya Kumar[1]

[1]HV Laboratory, Department of Electrical Engineering, Indian Institute of Science, Bangalore 560012, India

✉ *E-mail: satish@iisc.ac.in*

Abstract: A simple procedure to estimate series capacitance of a uniform transformer winding from its measured frequency response analysis (FRA) and shunt capacitance is presented. Unlike previously published approaches, this method does not involve any cumbersome and time-consuming curve-fitting nor running optimisation/search algorithms, and neither does it require data of winding geometry. The procedure relies on a property that is observable in the impedance function of a lossless winding, viz., the ratio of the product of squares of open circuit natural frequencies to the product of squares of short circuit natural frequencies bears a special relation to impedance function coefficients. Its feasibility was initially verified by simulation, and then by experiments on small-sized continuous-disk and interleaved-disc windings, followed by a large-sized 33 kV, 3.5 MVA continuous-disc winding, and finally on a 315 kVA 11/13.8 kV transformer. After measuring FRA, the process involves just finding roots of a polynomial, from which the initial impulse voltage distribution constant and series capacitance can directly be determined. Given these attractive features, authors believe that this method is implementable on existing FRA instruments, so that, along with routinely measured FRA, these two important constants of a winding can be displayed.

1 Introduction

Series capacitance (C_s) of transformer winding is a vital design parameter which along with the shunt capacitance governs the initial impulse voltage distribution when a surge impinges on it. Its value essentially conveys the net capacitive coupling offered by different disks/double-disks of the winding. Designers employ the well-established method of interleaving of individual turns to increase series capacitance and consequently achieve a more uniform initial impulse voltage distribution. Hence, knowledge of series capacitance is paramount for ascertaining or predetermining the winding's transient behaviour [1–4]. Although shunt capacitance is readily measurable, the same is not the case for series capacitance. Also, there exists no simple method to cross-check how closely was the intended design value of C_s actually realised after manufacture of the winding. Ideally speaking, it would be desirable to perform this cross-check on every manufactured winding, and preferably this check is based on measurements.

The other additional benefits that arise from C_s estimation are:

(a) Foremost, it acts as a cross-verification of the design data and proves how closely was the design value of C_s reproduced by the manufacturing process. Unfortunately, this cannot be determined by any other measurement-based method, other than by doing an initial impulse voltage distribution measurement which would require a sacrificial winding.
(b) Permits construction of a lumped-parameter ladder network equivalent circuit.
(c) Estimating C_s of existing windings can be now rendered possible by the proposed method when geometry and other winding data are unavailable, which is often the scenario.
(d) And more importantly, based on the recent work from the authors' research group [5], it is expected that C_s would also possess diagnostic capabilities similar to the quantity called equivalent air-core inductance of a winding.

These are the important reasons for estimating C_s, and in that context, the objective of this contribution is to devise a simple method to indirectly measure the series capacitance of a winding via the frequency response analysis (FRA) measurement.

2 Literature review

A brief summary of previous efforts directed towards estimation of series capacitance is given as follows:

1. Predetermination of the series capacitance of winding during its design stages was a much-discussed topic in the early 1950s–1960s, and all these efforts essentially pursued an analytical or semi-analytical approach, and required complete data on winding geometry, insulation data, clearances etc. [6–9]; a requirement not easily available to end-users. Many formulae were developed during that time period, but interestingly each one yielded a different result even for a given winding, and so it was arguable which one of them was more appropriate to use. In other words, there was no consensus amongst the developed methods. Moreover, each of these formulae was specific for a given type or structure of winding, and so needed to be entirely reworked when the design changed; which is not a trivial task.
2. In later years (1990s) researchers in [10–12] reported the use of finite element method (FEM) and charge simulation method (CSM) based approaches to predetermine C_s, but, as in early efforts, these also required data about winding geometry. Usually, this information is hard to get, and only available with manufacturers/designers. Even though in both these approaches series capacitance can be estimated, but there was no simple way to cross-verify them.
3. In the past decade or so, FRA has become a de facto monitoring tool of the power utilities to assess the mechanical integrity of the winding [13–16]. Keeping this in mind, the authors' research group successfully demonstrated the possibility of indirectly estimating C_s from measured FRA data, for both single and three-phase transformers [17, 18]. This was a major step forward. However, fitting an accurate

curve for measured FRA was a crucial and time-consuming step that needed special skills requiring some background knowledge and experience. This was its drawback that prevented its immediate deployment in industry. Some simplifications were suggested by authors in [19], but this approach was non-FRA-based, required additional instruments etc. Specifically, it was a time-domain approach that required exciting the winding by a nearly step-like waveform using a recurrent surge generator.

So, analysis of the published literature on the estimation of C_s leads to the following observation:

1. A direct measurement to estimate C_s is ruled out.
2. Also, there exists no simple approach for determining C_s from measured FRA that can be used by unskilled operators.
3. Consequently, it is imperative to explore alternative methods that would possess the following features:

    - be simple and easily implementable in software;
    - be implementable on existing FRA instruments as an add-on;
    - be based on FRA and any other terminal measurement;
    - avoid complexities like optimisation, curve-fitting etc.;
    - involve minimum post-processing after acquiring FRA data;
    - be applicable to all types of uniform windings.

Consequently, developing a method that possesses *ALL* the aforementioned features is the main objective of this paper.

3 Methodology

The underlying principle is initially presented for a lossless case. The losses in the winding are neglected [20] while formulating the method and later a method is suggested to overcome its effect. It was possible to put together a simple procedure by a deft manipulation and combination of a few well-known properties that correlate the roots of a polynomial to its coefficients. One special case of the Vieta's theorem [21] is exploited in its formulation. Details are discussed under the following subheadings.

3.1 Background

Consider an N-section, lossless, lumped-parameter, mutually coupled ladder-network model (as shown in Fig. 1) of a uniform transformer winding [3]. The model consists of per section series capacitance (C_s), per section shunt capacitance (C_g), per section self inductance (L_{ii}) and mutual inductance (L_{ij}) between any two sections. For representing frequency response, the driving point impedance (DPI) function is considered, since it possesses some unique properties like physical realisability, the alternating arrangement of poles and zeros etc. which are very useful in this work. In general, the DPI function for a lossless N-section ladder network (with its neutral open) can be written as [22]

$$\mathrm{DPI}(s) = \frac{a_0 s^{2N} + a_1 s^{2N-2} + \cdots + a_N}{b_0 s^{2N+1} + b_1 s^{2N-1} + \cdots + b_N s} \tag{1}$$

Let the numerator and denominator of DPI(s) be defined as follows:

$$P(s) = a_0 s^{2N} + a_1 s^{2N-2} + \cdots + a_N \tag{2}$$

$$Q(s) = b_0 s^{2N+1} + b_1 s^{2N-1} + \cdots b_N s \tag{3}$$

$Q(S)$ can be further rewritten as

$$\frac{Q(s)}{s} = (b_0 s^{2N} + b_1 s^{2N-2} + \cdots + b_N) \tag{4}$$

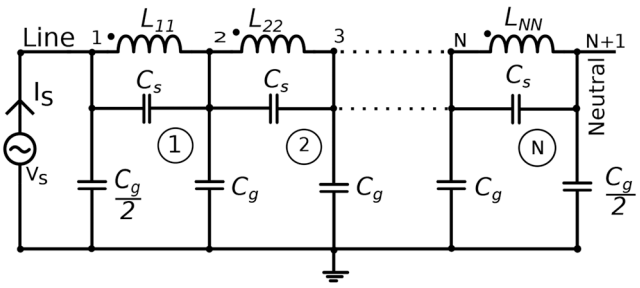

Fig. 1 *N-section mutually coupled ladder network*

Polynomials on the RHS of (2) and (4) are similar in structure but differ only in their coefficients. The following properties can be easily observed from these two polynomials:

1. The powers of 's' are always an even number, hence, they are both even polynomials. The number of sign changes for $P(s)$ and $P(-s)$ is zero. The same is true for $Q(s)/s$ as well. Hence, from Descartes' rule-of-signs [21] there exist no positive or negative real roots for these two expressions.
2. Since losses are neglected, all the roots of $P(s)$ and $Q(s)/s$ will be purely imaginary and shall exist as complex conjugate pairs. Let the roots of $P(s)$ be $\pm \mathrm{j}\omega_i'$ and all the non-zero roots of $Q(s)$ be $\pm \mathrm{j}\omega_i$. Obviously from the definition, since ω_i's are the roots of the numerator polynomial they correspond to the short circuit natural frequencies (scnf), and likewise, ω_is being roots of denominator polynomial correspond to the non-zero open circuit natural frequencies (ocnf) of the circuit under consideration. Furthermore, these ocnf and scnf correspond to the peaks and troughs in the DPI magnitude plot, respectively.

3.2 Linking roots of a polynomial to its coefficients

Next, some unique properties of such polynomials are invoked and then used subsequently to formulate the proposed method.

Property 1: If a new polynomial is constructed from a given polynomial by reversing the order of all the coefficients, then the roots of the new polynomial will be the multiplicative inverse of the roots of the original polynomial [21].

Property 2: Starting from an even polynomial, if a new polynomial is constructed by halving the powers of its variable without altering the coefficients, then the roots of the new polynomial will be square of the roots of an original polynomial [21].

Using these two properties, from $P(s)$ construct a new polynomial $P_1(s)$ such that the coefficients of $P(s)$ are reversed and the powers of 's' are halved, and that leads to

$$P_1(s) = a_N s^N + a_{N-1} s^{N-1} + \cdots + a_0 \tag{5}$$

Due to Properties 1 and 2, the roots of the new polynomial $P_1(s)$ will be $1/(\mathrm{j}\omega_i')^2$. Likewise, from (4), a new polynomial $Q_1(s)/s$ can be constructed as

$$\frac{Q_1(s)}{s} = (b_N s^N + b_{N-1} s^{N-1} + \cdots + b_0) \tag{6}$$

which would have its roots as $1/(\mathrm{j}\omega_i)^2$.

Property 3: (Vieta's Theorem): The symmetric sum of the roots of a polynomial is defined as those sums of roots which are unchanged by any permutation of these roots. There will be N symmetric sums for an Nth order polynomial and the pth elementary symmetric sum of a set of N roots is the sum of all products of p of those roots ($1 \le p \le N$). The symmetric sum of roots of polynomial is related with to polynomial coefficients, by the well-known Vieta's theorem [21], which states that, if we

Table 1 Expressions $((a_0/b_0)\cdot(b_N/a_N))$ in terms of $\gamma = C_g/C_s$, for different N

N	$(\frac{a_0}{b_0}\cdot\frac{b_N}{a_N})$
3	$\frac{2N(\gamma^3+6\gamma^2+9\gamma+2)}{\gamma^3+8\gamma^2+19\gamma+12}$
4	$\frac{2N(\gamma^4+8\gamma^3+20\gamma^2+16\gamma+2)}{\gamma^4+10\gamma^3+34\gamma^2+44\gamma+16}$
5	$\frac{2N(\gamma^5+10\gamma^4+35\gamma^3+50\gamma^2+25\gamma+2)}{\gamma^5+12\gamma^4+53\gamma^3+104\gamma^2+85\gamma+20}$
6	$\frac{2N(\gamma^6+12\gamma^5+54\gamma^4+112\gamma^3+105\gamma^2+36\gamma+2)}{\gamma^6+14\gamma^5+76\gamma^4+200\gamma^3+259\gamma^2+146\gamma+24}$
7	$\frac{2N(\gamma^7+14\gamma^6+77\gamma^5+210\gamma^4+294\gamma^3+196\gamma^2+49\gamma+2)}{\gamma^7+16\gamma^6+103\gamma^5+340\gamma^4+606\gamma^3+560\gamma^2+231\gamma+28}$

denote S_p as the pth elementary symmetric sum for polynomial $P_1(s)$, then we can write

$$S_p = (-1)^p \frac{a_{N-p}}{a_N} \quad p \in \{1, 2 \ldots N\} \tag{7}$$

Here, the value of p ranges from 1 to N. Hence, N such equations can be derived which relates the roots and coefficients of a DPI function. However, here we are considering a special case, wherein $p = N$. For the polynomial $P_1(s)$, if we consider $p = N$, then the Nth symmetric sum gives the product of all the roots of a polynomial $P_1(s)$. As $P_1(s)$ is the numerator of DPI (whose roots are the scnfs by definition), let this term be called Π_{scnf}, and can be written as:

$$\Pi_{\text{scnf}} = \frac{1}{(\mathrm{j}\omega_1')^2(\mathrm{j}\omega_2')^2\ldots(\mathrm{j}\omega_N')^2} = (-1)^N \frac{a_0}{a_N} \tag{8}$$

It is easy to observe that for both odd and even values of N, the negative sign gets cancelled on both the sides of (8) and hence can be simplified as

$$\Pi_{\text{scnf}} = \frac{1}{(\omega_1')^2(\omega_2')^2\ldots(\omega_N')^2} = \frac{a_0}{a_N} \tag{9}$$

And, similarly, for (6), we can write

$$\Pi_{\text{ocnf}} = \frac{1}{(\mathrm{j}\omega_1)^2(\mathrm{j}\omega_2)^2\ldots(\mathrm{j}\omega_N)^2} = (-1)^N \frac{b_0}{b_N} \tag{10}$$

Employing the same logic as above, it can be simplified as

$$\Pi_{\text{ocnf}} = \frac{1}{(\omega_1)^2(\omega_2)^2\ldots(\omega_N)^2} = \frac{b_0}{b_N} \tag{11}$$

Next, dividing (9) by (11), we get

$$\frac{\Pi_{\text{scnf}}}{\Pi_{\text{ocnf}}} \Rightarrow \frac{\omega_1^2\omega_2^2\ldots\omega_N^2}{\omega_1'^2\omega_2'^2\ldots\omega_N'^2} = \frac{a_0}{b_0}\cdot\frac{b_N}{a_N} \tag{12}$$

Taking this ratio is a crucial step in the formulation of the method that will become evident next. The LHS of (12) is a term that consists of entirely measurable quantities extractable from DPI magnitude plot. In other words, this quantity is *nothing but a ratio of the product of the squares of peak frequencies to the product of the squares of the trough frequencies*. On the other hand, the terms a_0, b_0, a_N and b_N on the RHS of (12) (being functions of the circuit elements) were computed for the network shown in Fig. 1, for different values of N, say, $N = 3, 4, 5, \ldots, 20$ using symbolic computation facility in MAPLE. It emerges that all these four terms are functions of C_g and/or C_s alone, for any N. The expressions corresponding to RHS of (12) can be nicely combined into a compact single expression in γ alone (viz., by substituting $\gamma = C_g/C_s$). For brevity, these are shown in Table 1, only for $N = 3$–7, as an example. From a study of these individual coefficients and its ratios (for different values of N), the following salient features can be observed:

1. For any value of N, the numerator and denominator of the ratio a_0/b_0 can be individually represented as a product of two terms; the first term is purely capacitive and the second term is purely inductive. Most importantly, the inductive term is common to both the numerator and denominator, and hence cancels out.
2. Writing DPI in normalised form b_N is a function of C_g alone and can be generalised as $4NC_g$, whereas, $a_N = 4$, always. Hence, $b_N/a_N = NC_g$. Since a ratio of the coefficients are taken, normalisation does not alter the final results.
3. Hence, the ratio $(a_0/b_0)\cdot(b_N/a_N)$ is always a function of C_g and C_s alone.
4. In the neutral open condition, there will be an equal number of non-zero peaks and troughs. So, LHS of (12) is a dimensionless quantity.
5. Thus, in compact form, we can write:

$$f(\gamma) = \frac{\Pi_{\text{scnf}}}{\Pi_{\text{ocnf}}} \tag{13}$$

Which in turn can, in general, be written as

$$2N\left(\sum_{i=0}^{N}\delta_i\gamma^i\right)\Big/\left(\sum_{i=0}^{N}\beta_i\gamma^i\right) = \frac{\Pi_{\text{scnf}}}{\Pi_{\text{ocnf}}} \tag{14}$$

where δ_i and β_i are the corresponding coefficients of numerator and denominator polynomials of $f(\gamma)$, respectively. For brevity, both these coefficients are shown in Tables 2 and 3 up to $N = 17$. However, these can be computed and stored for any desirable higher value of N if required. Once the numerical value of $\Pi_{\text{scnf}}/\Pi_{\text{ocnf}}$ is computed from measured DPI, solving (14) directly leads to the value of γ. Since the value of C_s and C_g cannot be negative, so the value of γ should always be positive. So, before solving (14), the existence of a positive real root can be ascertained using Descartes' rule-of-signs. The total shunt capacitance of a transformer winding can be measured by an LCR meter. So, using this measured value and computed γ, the value of C_s can be estimated.

3.3 Existence of ONLY one positive real root of $f(\gamma)$

At this juncture, it might be worth mentioning that a proof to show the existence of only one positive real root of the equation $f(\gamma)$ was undertaken (see Appendix 1). For brevity, only the important point is mentioned here:

Substituting $\Pi_{\text{scnf}}/\Pi_{\text{ocnf}} = k$, rearranging and simplifying (14) yields

$$\begin{aligned}(2N-k)\gamma^N + (2N\delta_{N-1} - k\beta_{N-1})\gamma^{N-1} \\ +\cdots+(2N\delta_0 - \beta_0 k) = 0\end{aligned} \tag{15}$$

Plugging in values of β_0 and δ_0 from Tables 2 and 3 results in

$$\begin{aligned}(2N-k)\gamma^N + \beta_{N-1}\left(2N\frac{\delta_{N-1}}{\beta_{N-1}} - k\right)\gamma^{N-1} \\ +\cdots\beta_0(1-k) = 0\end{aligned} \tag{16}$$

In DPI magnitude plot when neutral is open, for any pair of $\omega_i - \omega_i'$, it is obvious that always $\omega_i > \omega_i'$. This arises from the basic fact that an scnf always precedes an ocnf, as can be verified in the DPI plot. This condition translates to the fact that 'k' will always be greater than 1. So, the last term $\beta_0(1-k)$ in (16) is always negative. The sign of the first term in (16) depends on the value of k. If the value of k lies between 1 and $2N$, then first term will be always positive. If $k > 2N$, the sign of first term will be

Table 2 Values of δ_i for different values of N, Note: $\delta_0 = 2$, and $\delta_N = 1$ for all N

N	γ^{16}	γ^{15}	γ^{14}	γ^{13}	γ^{12}	γ^{11}	γ^{10}	γ^{9}	γ^{8}	γ^{7}	γ^{6}	γ^{5}	γ^{4}	γ^{3}	γ^{2}	γ^{1}
3														1	6	9
4													1	8	20	16
5												1	10	35	50	25
6											1	12	54	112	105	36
7										1	14	77	210	294	196	49
8									1	16	104	352	660	672	336	64
9								1	18	135	546	1287	1782	1386	540	81
10							1	20	170	800	2275	4004	4290	2640	825	100
11						1	22	209	1122	3740	8008	11,011	9438	4719	1210	121
12					1	24	252	1520	5814	14,688	24,752	27,456	19,305	8008	1716	144
13				1	26	299	2002	8645	25,914	50,388	68,952	63,206	37,180	13,013	2366	169
14			1	28	350	2576	12,397	40,964	94,962	155,040	176,358	136,136	68,068	20,384	3185	196
15		1	30	405	3250	17,250	63,756	168,245	319,770	436,050	419,900	277,134	119,340	30,940	4200	225
16	1	32	464	4032	23,400	95,680	283,360	615,296	980,628	1,136,960	940,576	537,472	201,552	45,696	5440	256
17	34	527	4930	31,059	139,230	457,470	1,118,260	2,042,975	2,778,446	2,778,446	1,998,724	999,362	329,460	65,892	6936	289

Table 3 Values of β_i for different values of N, Note: $\beta_0 = 4N$, and $\beta_N = 1$ for all N

N	γ^{16}	γ^{15}	γ^{14}	γ^{13}	γ^{12}	γ^{11}	γ^{10}	γ^{9}	γ^{8}	γ^{7}	γ^{6}	γ^{5}	γ^{4}	γ^{3}	γ^{2}	γ^{1}
3														1	8	19
4													1	10	34	44
5												1	12	53	104	85
6											1	14	76	200	259	146
7										1	16	103	340	606	560	231
8									1	18	134	532	1210	1572	1092	344
9								1	20	169	784	2171	3652	3630	1968	489
10							1	22	208	1104	3605	7462	9724	7656	3333	670
11						1	24	251	1500	5644	13,888	22,477	23,452	15,015	5368	891
12					1	26	298	1980	8436	24,072	46,648	60,944	52,195	27,742	8294	1156
13				1	28	349	2552	12,145	39,444	89,148	140,352	151,606	108,680	48,763	12,376	1469
14			1	30	404	3224	16,951	61,754	159,600	294,576	385,662	350,948	213,928	82,160	17,927	1834
15		1	32	463	4004	23,050	93,104	270,963	574,332	885,666	981,920	764,218	401,336	133,484	25,312	2255
16	1	34	526	4900	30,654	135,980	440,220	1,054,504	1,874,730	2,458,676	2,342,396	1,578,824	722,228	210,120	34,952	2736
17	36	593	5920	39,991	193,284	689,130	1,841,840	3,712,775	5,633,804	6,374,082	5,281,696	3,115,658	1,253,240	321,708	47,328	3281

always negative. The existence of a single positive root for both these conditions of k is discussed in Appendix 1. From the proof, it emerges that *'if the value of k is less than* 2*N, then there will always exist a single positive root for (16)'*. For each case, before finding the roots, this check is made.

3.4 Salient features

This procedure for estimation of C_s has the following advantages compared to all other previously published methods in the literature:

1. The entire DPI data need not be processed, but, only data points pertinent to the peaks and troughs are required. In addition, the measured value of total shunt capacitance is the only other data required.
2. No curve-fitting or optimisation exercise is required. In practical DPI measurements, it is often observed that a dominant pole tends to mask nearby non-dominant poles and these have to be carefully considered during curve-fitting. Hence, fitting DPI magnitude is invariably a task that calls for mathematical skills and experience. This is completely avoided in the proposed method.
3. From the point of implementation on an FRA instrument, the proposed method is very simple and elegant. It only requires a lookup table for storing the δ_i and β_i coefficients (a one-time exercise) and a simple algorithm for finding roots. Hence, the proposed method is ideally suited for use in factories, as well as, in laboratories.
4. The initial impulse voltage distribution constant, popularly termed as α of the winding, is the ratio of the square root of the total shunt to the total series capacitance, and can readily be computed from γ using

$$\alpha = N\sqrt{\gamma}\,. \tag{17}$$

Finally, it is important to highlight here that α can be calculated without measuring either C_g or C_s explicitly. To the best of authors' knowledge, this is the first time an indirect measurement-based method is proposed for determining α without the explicit knowledge of either C_g or C_s.

3.5 Limitation of method and means to overcome it

The analytical formulation of the proposed method was built around the assumption that losses in a transformer winding are small enough to be ignored. This is far from true, especially at the higher frequencies, which makes its implementation questionable. This issue arises from the fact that this method presumes peak-trough pair values as extracted from the DPI magnitude are the true value of pole-zero; this is true, if and only if, the losses are negligible. However, when losses become significant at higher frequencies, the peak-trough pairs as observed from the magnitude plot WILL NO LONGER COINCIDE with the true value of pole-zero, and hence they cannot be directly determined by extracting it from the DPI magnitude plot. Thus, the method will begin to yield erroneous results. To overcome this limitation, authors propose to extract and use all peak-trough pairs that lie below a frequency

Table 4 Self and mutual inductance between first and ith section

mH	L_{11}	L_{12}	L_{13}	L_{14}	L_{15}	L_{16}
L	1.00	0.7408	0.5488	0.4066	0.3012	0.2231

mH	L_{17}	L_{18}
L	0.1653	0.1225

Table 5 Peak-trough pairs corresponding to Fig. 2

Mrad/s	1	2	3	4	5	6
ω_i'	0.1936	0.6995	1.3198	1.9453	2.5169	2.9923
ω_i	0.3450	0.8426	1.4052	1.9911	2.5380	3.0018

Mrad/s	7	8
ω_i'	3.3473	3.5660
ω_i	3.3508	3.5670

Table 6 Peak-trough pairs corresponding to Fig. 3

Mrad/s	1	2	3	4	5	6
ω_i'	0.1936	0.6995	1.3194	1.9426	2.5072	2.9743
ω_i	0.3450	0.8426	1.4057	1.9937	2.5476	3.0199

Mrad/s	7	8
ω_i'	3.3252	3.5529
ω_i	3.3728	3.5805

limit of about 2–2.5 Mrad/s, wherein the presumption is still largely applicable. The real part of the pole or zero is very small to be safely ignored in this frequency interval, a fact which was confirmed by curve-fitting exercise. Most importantly, the imposition of this bound permits implementation of the method as it is. Ignoring higher frequency peak-trough pairs does not seriously affect end results (as will become evident later), compared to the scenario of including all peak-trough pairs which leads to unacceptable errors. This modified approach is used.

(*Note:* The method was initially developed for a lossless case since it is easy to describe, explain and cross-check. Furthermore, losses in a transformer winding are usually very small and can be neglected for practical purposes at lower frequencies. However, when frequency increases, they tend to become significant and cannot be ignored. For this reason, the proposed method had to be modified to consider the defined ratio of Π_{scnf}/Π_{ocnf} ONLY up to a certain frequency limit. The objective was to develop a simple, and easily implementable method which can be deployed on existing FRA measuring instrument. Hence, this simplification was proposed so that the method is applicable without or with losses).

4 Simulation

Initially, the proposed procedure was checked by simulation studies using an eight-section ($N = 8$) mutually coupled ladder network, as shown in Fig. 1. Since all the parameters of this network are known, the capability of the proposed steps can be judged. The elements of the network used were $C_s = 0.444\,\text{nF}$ and $C_g = 0.25\,\text{nF}$, which corresponds to $\alpha = 6$. The self-inductance of the first section and mutual inductances between 1st and ith section are given in Table 4. Symmetry considerations are invoked for determining the rest of them. Initially, a lossless case is considered, followed by a lossy case modeled by a series resistance of 10 Ω/section.

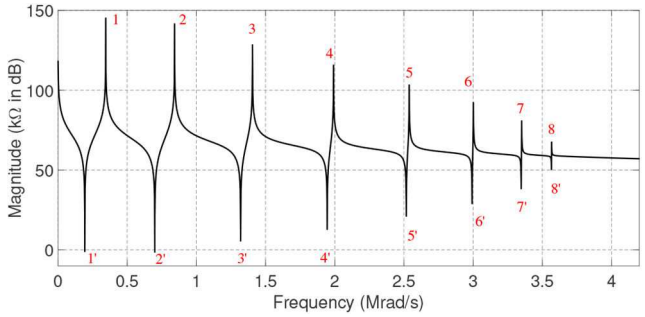

Fig. 2 *Computed DPI magnitude response of a mutually coupled ladder network without losses*

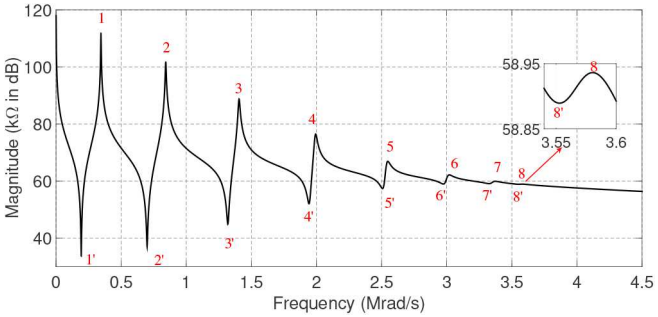

Fig. 3 *Computed DPI magnitude response of a mutually coupled ladder network with losses*

4.1 Without loss

After plugging in all these values into a circuit simulation software (PSpice), the DPI magnitude was determined by performing AC-analysis, and is shown in Fig. 2. The peak-trough pairs outputted by Matlab program '*findpeaks*' are marked on Fig. 2 and the same is also tabulated in Table 5. Steps for computing C_s are as follows:

1. Number of peak-trough pairs were found to be eight, so $N = 8$.
2. Picking up all peak-trough pairs (shown in Table 5), yields $\Pi_{scnf}/\Pi_{ocnf} = 5.6175$.
3. The pertinent $f(\gamma)$ is

$$10.4\gamma^8 + 154.9\gamma^7 + 911.3\gamma^6 + 2643.5\gamma^5 + 3762.8\gamma^4 + 1921.3\gamma^3 - 758.3\gamma^2 - 908.4\gamma - 147.8 = 0 \quad (18)$$

4. Solving (18) yields $\gamma = 0.5624$.
5. So, $\alpha = 5.9995$. This corresponds to $C_s = 0.4445\,\text{nF}$, which closely matches its true value of 0.444 nF.

4.2 With loss

Loss was considered by inserting a resistance of 10 Ω/section in series with the inductor. The above computations are repeated. The DPI magnitude plot is shown in Fig. 3, along with the peak-trough pairs in Table 6. Steps to compute C_s are as follows:

1. Number of peak-trough pairs were found to be eight, so $N = 8$.
2. Picking up all peak-trough pairs (shown highlighted) which are below 2.5 Mrad/s, yields $\Pi_{scnf}/\Pi_{ocnf} = 5.6920$.
3. The pertinent $f(\gamma)$ is (see (19)) .

$$10.3080\gamma^8 + 153.5440\gamma^7 + 901.2717\gamma^6 + 2603.9\gamma^5 + 3672.7\gamma^4 + 1804.2\gamma^3 - 839.6668\gamma^2 - 934.0489\gamma - 150.1441 = 0 \quad (19)$$

4. Solving (19) yields $\gamma = 0.5796$, which corresponds to $\alpha = 6.0905$.
5. This implies $C_s = 0.4313$ which closely matches its true value.
6. Thus, even when losses are present, the procedure can be used.

5 Implementation on uniform transformer windings

Triggered by the success of the proposed method in simulation studies, the next step was to examine its applicability on uniform transformer windings. In all these experiments, DPI was measured by manually sweeping the frequency and measuring the response (viz., input current) at each discrete frequency step. The instruments used for this were as follows:

- A 0–20 V_{p-p}, 0–60 MHz, function generator.
- A 2 mV/mA current probe with bandwidth 450 Hz–60 MHz.
- An 8-bit, 200 M samples/s digital oscilloscope.

During DPI measurement, as sine waves are being measured, elimination of noise was achieved by using 'averaging option' available on the digital oscilloscope. Furthermore, at each measurement the vertical amplitude of the channel measuring current was dynamically adjusted so that the measured waveform always occupies >90% of the full-scale amplitude of the channel; this guarantees a high signal-to-noise ratio. (*Note:* The achievable accuracy of the proposed method significantly depends on our ability to accurately identify and extract the DPI magnitude peaks and troughs. So, all the above-mentioned efforts were exercised to attain the maximum possible signal-to-noise ratio and hence achieve the highest possible accuracy.) Initially, experiments were performed on single isolated continuous-disc and interleaved-disc windings. Then, the method is examined on an actual two-winding single-phase testing transformer. Details of each case is presented below.

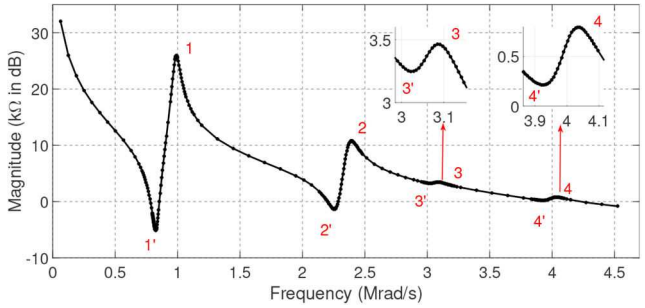

Fig. 4 *Measured DPI magnitude response of a single isolated fully interleaved-disc winding*

Table 7 Peak-trough pairs corresponding to Fig. 4

Mrad/s	1	2	3	4
ω_i'	0.8225	2.2563	3.0159	3.9207
ω_i	0.9896	2.3952	3.0788	4.0338

Table 8 Peak-trough pairs corresponding to Fig. 5

Mrad/s	1	2	3	4	5
ω_i'	0.4511	1.1592	1.8341	2.5258	3.1994
ω_i	0.8394	1.3628	2.0395	2.7219	3.3879

Mrad/s	6	7	8
ω_i'	3.9333	4.5302	5.3533
ω_i	4.1532	4.7375	5.5543

5.1 Case A: single, isolated, fully interleaved-disc winding

A uniform fully interleaved-disc winding was chosen which had 16 discs with 10 turns per disc. The paper insulated copper turn has a cross-section area of 30 mm^2. The winding had a height of 215 mm, and inner and outer diameters of 260 and 350 mm, respectively. The insulation thickness, duct spacing etc. corresponded to an 11 kV rating. An aluminum sheet was concentrically placed to simulate the ground plane. (*Note:* The DPI of ONLY a linear system can be defined. In the frequency interval of 10 kHz–1 MHz, the winding behaves as a linear element, since the iron core repels almost all the flux due to eddy currents and in turn, the winding offers a constant inductance value (equivalent to an air-core inductance). Keeping this scenario in mind, the iron core which acts as a magnetic shield in this frequency interval was emulated by a grounded aluminium cylinder.) The measured DPI plot is shown in Fig. 4. The peak-trough pairs were found by 'findpeaks' and they are marked on it for clarity. These frequencies are also tabulated in Table 7. The steps for estimating C_s are as follows:

1. Peak-trough pairs in DPI magnitude were four, hence $N = 4$.
2. Picking up the first two peak-trough pairs (which are below 2.5 Mrads/s) in Table 7, compute $\Pi_{scnf}/\Pi_{ocnf} = 1.6313$.
3. Using coefficients in Tables 2 and 3 for $N = 4$, $f(\gamma)$ is constructed and equated to Π_{scnf}/Π_{ocnf}. The simplified expression is

$$6.3686\gamma^4 + 47.6861\gamma^3 + 104.5329\gamma^2 + 56.2190\gamma - 10.1022 = 0 \quad (20)$$

4. Since $\Pi_{scnf}/\Pi_{ocnf} < 2N$, there will exist ONLY one positive real root for (20).
5. Using the positive root of $\gamma = 0.1406$, the value of α was computed as 1.4996. This low value of α is a characteristic feature of a fully interleaved-disc winding.
6. The measured value of total shunt capacitance was 0.410 nF at 1 kHz, so shunt capacitance per section is $C_g = 0.1025$ nF. Estimated series capacitance per section was $C_s = 0.7290$ nF.

5.2 Case B: 2.2 kV continuous-disc winding in presence of a shorted LV winding

One healthy phase of an HV winding (along with an inner LV winding) was scavenged from an old discarded transformer. It was one of the phases of a $\Delta - Y$ transformer of rating 70 kVA, 2200/220 V, 25 Hz. (*Note:* It is well-known that the measured DPI would be modified due to the presence of a shorted secondary winding, in addition to other surrounding conditions, other neighbouring windings, terminal condition of all non-tested windings etc. However, the value of C_s of the excited winding, which would be extracted from the measured DPI, will remain unchanged. This fact has been previously examined in [18] and proved.) An aluminium sheet was concentrically placed inside the LV winding which emulates the presence of core. The non-tested LV winding is shorted and connected to the aluminium sheet. The DPI magnitude was measured and the peak-trough pairs are extracted and tabulated in Table 8. The DPI magnitude plot is shown in Fig. 5, and also contains markings of each peak-trough pair.

1. DPI magnitude plot has eight peak-trough pairs, so, $N = 8$.
2. From the first three peak-trough pairs which are below 2.5 Mrads/s, $\Pi_{scnf}/\Pi_{ocnf} = 5.9172$.
3. Using coefficients in Tables 2 and 3 corresponding to $N = 8$, the polynomial $f(\gamma)$ was constructed and equated to Π_{scnf}/Π_{ocnf}. The simplified expression is

$$10.1\gamma^8 + 149.5\gamma^7 + 871.1\gamma^6 + 2484\gamma^5 + 3400.1\gamma^4 + 1450.1\gamma^3 - 1085.6\gamma^2 - 1011.5\gamma - 157.4 = 0 \quad (21)$$

4. Since $\Pi_{scnf}/\Pi_{ocnf} < 2N$hence there exists ONLY one positive real root for (21).
5. After solving (21), the only positive root of $\gamma = 0.6338$.
6. The corresponding value of $\alpha = 6.3687$.
7. The measured total shunt capacitance was 0.6904 nF at 1 kHz, so shunt capacitance per section is $C_g = 0.0863$ nF. Hence, the estimated series of capacitance per section is $C_s = 0.1362$ nF.

5.3 Case C: 33 kV, 3.5 MVA, continuous-disc winding

Next, experiments were done on another uniform single isolated continuous-disc winding manufactured specifically for this purpose. This was one of the HV windings of a new 3-Φ, 33 kV, 3.5 MVA transformer. The winding had 24 number of double-discs with 22 turns per disc. Its total height was 570 mm. Spacing between each disc is 3 mm, and the inner and outer diameters of each disc is 395 and 486 mm, respectively. An aluminium sheet was concentrically placed to simulate the ground plane. Measured DPI magnitude is shown in Fig. 6. The peak-trough pairs outputted by 'findpeaks' are tabulated in Table 9.

1. From DPI magnitude plot, the number of peak-trough pairs are 14. Hence $N = 14$.
2. From the first four peak-trough pairs that are below 2.0 Mrads/s, $\Pi_{scnf}/\Pi_{ocnf} = 10.8246$.
3. Using the coefficients in Tables 2 and 3 corresponding to $N = 14$, the polynomial $f(\gamma)$ was constructed and equated to Π_{scnf}/Π_{ocnf}. The simplified expression is

$$\begin{aligned} &17.1754\gamma^{14} + 459.261\gamma^{13} + 5426.9\gamma^{12} + 3.7229 \times 10^4\gamma \\ &+1.6363 \times 10^5\gamma^{10} + 4.7853 \times 10^5\gamma^9 + 9.3133 \times 10^5 \\ &+1.1524 \times 10^6\gamma^7 + 7.6338 \times 10^5\gamma^6 + 1.2928 \times 10^4\gamma (22) \\ &-4.0979 \times 10^5\gamma^4 - 3.1860 \times 10^5\gamma^3 - 1.0487 \times 10^5\gamma \\ &-1.4364 \times 10^4\gamma - 550.1790 = 0 \end{aligned}$$

4. Since $\Pi_{scnf}/\Pi_{ocnf} < 2N$, there exist ONLY one positive real root for (22).
5. The only positive root of γ is 0.7029.
6. This corresponds to an estimated value of $\alpha = 11.7375$. This is a typical value of α that corresponds to continuous disc winding.
7. The measured total shunt capacitance is 1.15 nF at 1 kHz, hence shunt capacitance per section $C_g = 0.0821$ nF. The estimated series capacitance per section is $C_s = 0.1169$ nF. So, the total series capacitance is 0.0083 nF.

5.3.1 Verification by initial impulse voltage distribution: As it is well-known that there is no direct method to verify the correctness of the estimated C_s, the authors measured the initial impulse voltage distribution and compare it with the one computed using the above-estimated value of C_s. This measurement was carried out by exciting the winding by a near-step-like (70 V, 0.27/36 µs) impulse voltage waveform produced using Haefely's repetitive surge generator (RS482). The voltage magnitude at each double-disk junction was measured corresponding to the time instant at which the input excitation is maximum. Plotting these voltages leads to the initial impulse voltage distribution, which is shown in Fig. 7, along with that computed using estimated $C_s = 0.1169$ nF. The close match of estimated and measured distributions goes to show that the proposed method has satisfactorily estimated the value of C_s.

5.3.2 Verification by CSM: One more way of verifying the estimated C_s was explored. Since, in this particular case, the authors had access to design data (physical dimensions of the winding are given in Fig. 8) this gave an opportunity to compute C_s using CSM, and it in-turn can be used to cross-verify the results gotten from the proposed method. The computation procedure and algorithm described in [12] was followed. As per this procedure, initially, the turn-to-turn capacitance matrix of the winding is computed. Then, capacitance between neighbouring discs (inter-disc capacitances) is obtained by adding the capacitances existing between all the turns in neighbouring discs. Finally, the series combination of all the disc capacitances provides the net series

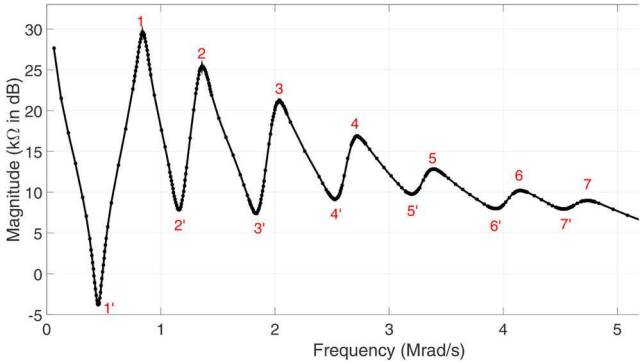

Fig. 5 *Measured DPI magnitude response of a 2.2 kV, continuous-disc winding in the presence of a shorted LV*

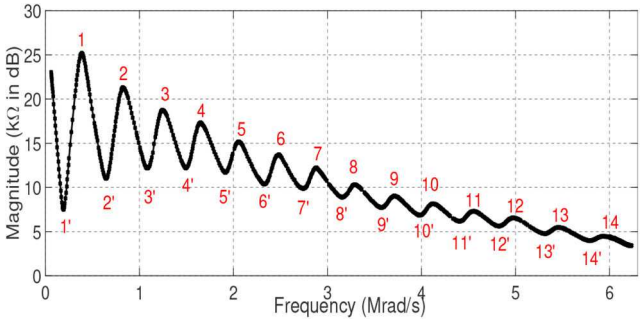

Fig. 6 *Measured DPI magnitude response of a single, isolated, 33 kV, 3.5 MVA, continuous-disc winding*

Table 9 Peak-trough pairs corresponding to Fig. 6

Mrad/s	1	2	3	4	5	6
ω_i'	0.1923	0.6447	1.0795	1.4941	1.9151	2.3292
ω_i	0.3889	0.8237	1.2428	1.6518	2.0546	2.4844

Mrad/s	7	8	9	10	11	12
ω_i'	2.7426	3.1542	3.5770	3.9747	4.4045	4.8255
ω_i	2.8840	3.2899	3.7096	4.1281	4.5553	4.9763

Mrad/s	13	14
ω_i'	5.3093	5.7931
ω_i	5.4601	5.9313

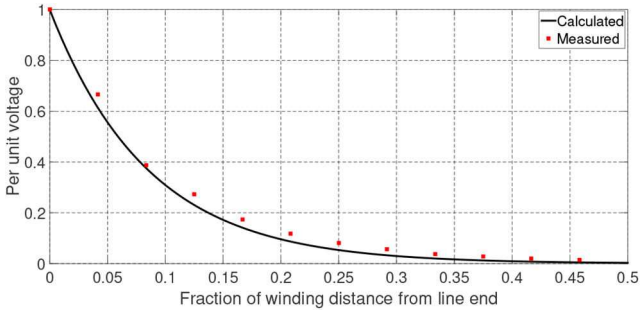

Fig. 7 *Measured and calculated initial impulse voltage distribution of 33 kV, 3.5 MVA, continuous disc winding*

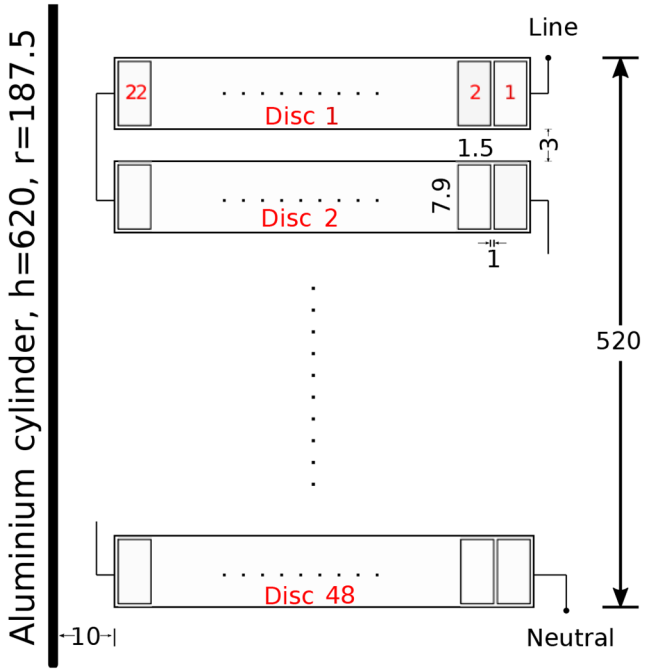

Fig. 8 *Dimensions of 33 kV, 3.5 MVA continuous-disc winding. All dimensions are in mm, and figure is not to scale. (Disc inner radius = 197.5, Disc outer radius = 243)*

Fig. 9 *Experimental set up to measure DPI on 13.8 kV winding of 11/13.8 kV, two-winding transformer with a center-tap*

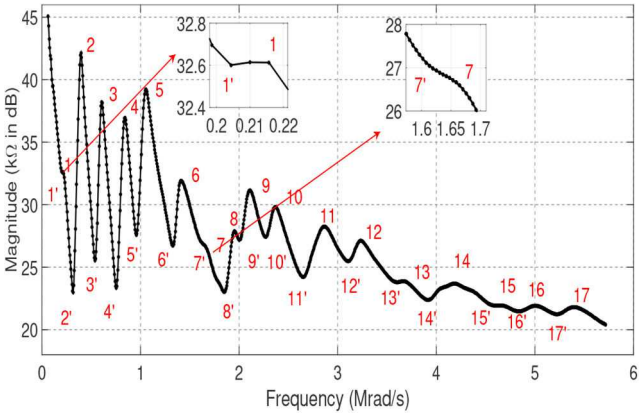

Fig. 10 *Measured DPI magnitude of the 13.8 kV winding of the 11/13.8 kV, two-winding transformer*

capacitance of the winding. The results obtained from CSM are enumerated as follows:

1. The net series capacitance is $C_s = 0.0099$ nF.
2. The net shunt capacitance is $C_g = 1.4478$ nF.
3. Thus, α is 12.0841, and is reasonably close to 11.7375 which was estimated by the proposed method.

Table 10 Peak-trough pairs corresponding to Fig. 10

Mrad/s	1	2	3	4	5	6
ω_i'	0.2043	0.3176	0.5383	0.7534	0.9572	1.3251
ω_i	0.2100	0.3968	0.6062	0.8440	1.0534	1.4100

Mrad/s	7	8	9	10	11	12
ω_i'	1.614	1.8516	2.0044	2.2704	2.6497	3.1082
ω_i	1.6590	1.9534	2.1120	2.3667	2.8648	3.2327

Mrad/s	13	14	15	16	17
ω_i'	3.6006	3.9176	4.5969	4.8347	5.2252
ω_i	3.6629	4.1837	4.6422	5.0045	5.3951

Hence, the accuracy of the proposed method was cross-verified by two independent indirect methods and found to be satisfactory.

5.4 Case D: experiment on 1 – Φ, two-winding transformer

Owing to the encouraging performance of the proposed method on single isolated windings, the next objective was to validate the proposed method on an actual two-winding transformer. For this purpose, a 1 – Φ, two-winding transformer of rating 11/13.8 kV, 315 kVA, used for testing surge-arrester blocks, was selected. When measuring DPI of one winding, the untested winding is kept open-circuited and floating. A photo of the experimental setup is shown in Fig. 9. (*Note:* In this particular case, the DPI was measured using a commercial impedance analyser (model PSM3750). The excitation signal was connected to line-terminal of the 13.8 kV winding and the neutral end was kept floating. Likewise, the secondary was kept open and floating. The input was fed with respect to the tank. The input voltage and source current are automatically measured at each frequency point and outputted.) The measured DPI is shown Fig. 10. The peak-trough pairs are extracted and the same are also tabulated in Table 10. The steps for estimating C_s are as follows:

1. After zooming DPI magnitude plot, a number of peak-trough pairs were counted to be 17. Hence, $N = 17$.
2. From first 9 peak-trough pairs (which are below 2.0 Mrads/s), $\Pi_{scnf}/\Pi_{ocnf} = 4.6991$.
3. Using the coefficients in Tables 2 and 3 corresponding to $N = 17$, the polynomial $f(\gamma)$ was constructed and equated to Π_{scnf}/Π_{ocnf}. The simplified expression is (see (23)) .
4. Since $\Pi_{scnf}/\Pi_{ocnf} < 2N$, hence there exists ONLY one positive real root for (23).
5. After solving (23), the only positive root of $\gamma = 0.0779$
6. The corresponding value of $\alpha = 4.7439$.
7. The measured shunt capacitance is 1.3 nF at 1 kHz, shunt capacitance per section $C_g = 0.0765$ nF. The estimated series capacitance per section is $C_s = 0.9820$ nF.

6 Implementability on existing FRA instruments

Given the simplicity of the proposed method, the authors foresee its portability on commercial FRA instrument to be straightforward. The expected major steps/aspects in that regard are listed as follows:

- The DPI magnitude data is acquired in a normal fashion.
- The peak-trough detection algorithm used in this work can be converted and ported into the instrument software. This algorithm always detected the peak-trough pairs accurately, except in one case, wherein peak-trough 7–7′ in Fig. 10 was not detected. Thus, this algorithm is robust and can be used.

$$
\begin{aligned}
&29.3009\gamma^{17} + 986.8319\gamma^{16} + 1.5131 \times 10^{4}\gamma^{15} \\
&+1.3980 \times 10^{5}\gamma^{14} + 8.6808 \times 10^{5}\gamma^{13} + 3.8256 \times 10^{6}\gamma^{12} \\
&+1.2316 \times 10^{7}\gamma^{11} + 2.9366 \times 10^{7}\gamma^{10} + 5.2014 \times 10^{7}\gamma^{9} \\
&+6.7993 \times 10^{7}\gamma^{8} + 6.4515 \times 10^{7}\gamma^{7} + 4.3137 \times 10^{7}\gamma^{6} \\
&+1.9337 \times 10^{7}\gamma^{5} + 5.3125 \times 10^{6}\gamma^{4} + 7.2859 \times 10^{5}\gamma^{3} \\
&+1.3424 \times 10^{4}\gamma^{2} - 5.5918 \times 10^{3}\gamma - 251.5397 = 0
\end{aligned} \tag{23}
$$

- Once all peak-trough pairs are identified, N is determined.
- Then, Π_{scnf}/Π_{ocnf} can be determined using all peak-trough pairs that are below the upper bound of 2–2.5 Mrads/s.
- From the stored lookup table, pertinent δ_i and β_i for a given N are used to construct the polynomial $f(\gamma)$.
- A check whether $\Pi_{scnf}/\Pi_{ocnf} < 2N$ is necessary to ensure the presence of a single positive real root.
- To find roots, the bisection method is a good option to use. An initial guess for the root has to be set. For this purpose, as only the positive root is required, the initial interval for γ can be set as 0–5.
- The convergence criterion can be set as 0.001.
- *Note:* This bisection algorithm was implemented and run on all the cases discussed in the previous section. In all runs, the positive root was estimated accurately in less than a few seconds. Thus, this method of finding roots is a satisfactory choice.
- Authors expect instrument manufacturers to implement this feature as an add-on option. This being a software addition, it can be retro-fitted.

7 Conclusions

A simple and elegant procedure for estimating series capacitance of a uniform transformer winding from measured frequency response data was presented. The theoretical aspects of the proposed method were derived by exploiting properties that correlate the roots of a polynomial to its coefficients. Invoking these properties on driving-point-impedance function of a winding (modelled as a N-section mutually coupled ladder network) led to the establishment of the proposed procedure. The method was implemented on a variety of uniform transformer windings to check its feasibility. Finally, it was also successfully implemented on an actual single-phase, two-winding transformer. All these experimental results prove its feasibility. The proposed method is free from mathematical complexities, is straightforward to implement, is time-efficient and therefore ideally suited to be deployed on existing commercial FRA instruments, as a software add-on option. This feature is expected to add a new dimension to the FRA instruments.

8 References

[1] Blume, L.F., Boyajian, A.: 'Abnormal voltages within transformers', *Transactions of the American Institute of Electrical Engineers*, 1919, **XXXVIII**, pp. 577–620

[2] Teranishi, T., Ikeda, M., Honda, M., *et al.*: 'Local voltage oscillation in interleaved transformer windings', *IEEE Trans. Power Appar. Syst.*, 1981, **100**, (2), pp. 873–881

[3] Heller, B., Veverka, A.: '*Surge phenomena in electrical machines*' (Iliffe Books, London, 1968, Revised English edn.)

[4] De, S., De, A., Bandyopadhyay, G.: 'Self-capacitance grading approach to suppress winding resonance in EHV transformers under oscillatory terminal disturbances', *IET High Voltage*, 2018, **3**, (4), pp. 310–315

[5] Mukherjee, P., Satish, L.: 'Estimating the equivalent air-cored inductance of transformer winding from measured FRA', *IEEE Trans. Power Deliv.*, 2018, **33**, (4), pp. 1620–1627

[6] Jayaram, B.N.: 'Bestimmung der stosspannungsverteilung in transformatoren mit digitalrechner', *ETZ-A*, 1961, **82**, pp. 1–9

[7] Waldvogel, P., Rouxel, M.: 'Predetermination by calculating of the electrical stresses in a winding subjected to a surge voltage'. CIGRE-Rep., 1956, 125

[8] Chowdhuri, P.: 'Calculation of series capacitance for transient analysis of winding', *IEEE Trans. Power Deliv.*, 1987, **2**, (1), pp. 133–139

[9] Popović, L.M.: 'New method for calculation of series capacitance for transient analysis of windings'. Proc. 9th Mediterranean Electrotechnical Conf., Tel-Aviv, Israel, 1998, vol. 2, pp. 1042–1046

[10] Bjerkan, E., Hoidalen, H.K.: 'High frequency FEM-based power transformer modelling: investigation of internal stresses due to network initiated over voltages', *Elect. Power Syst. Res.*, 2007, **77**, pp. 1483–1489

[11] Zhang, Z.W., Tang, W.H., Ji, T.Y., *et al.*: 'Finite-element modelling for analysis of radial deformations within transformer windings', *IEEE Trans. Power Deliv.*, 2014, **29**, (5), pp. 2297–2305

[12] de Leon, F., Semlyen, A.: 'Efficient calculation of elementary parameters of transformers', *IEEE Trans. Power Deliv.*, 1992, **7**, (1), pp. 376–383

[13] Dick, E.E., Erven, C.C.: 'Transformer diagnostic testing via frequency response analysis', *IEEE Trans. Power Appar. Syst.*, 1978, **97**, (6), pp. 2144–2153

[14] Steven Mitchell, D., James Welsh, S.: 'Methodology to locate and quantify radial winding deformation in power transformers', *IET High Voltage*, 2017, **2**, (1), pp. 17–24

[15] Samimi, M.H., Tenbohlen, S., Shayegani Akmal, A.A., *et al.*: 'Evaluation of numerical indices for the assessment of transformer frequency response', *IET Gener. Transm. Distrib.*, 2017, **11**, (1), pp. 218–227

[16] Gomez-Luna, E., Aponte Mayor, G., Gonzalez-Garcia, C., *et al.*: 'Current status and future trends in frequency-response analysis with a transformer in service', *IEEE Trans. Power Deliv.*, 2013, **28**, (2), pp. 1024–1031

[17] Pramanik, S., Satish, L.: 'Estimation of series capacitance of a transformer winding based on frequency-response data: an indirect measurement approach', *IEEE Trans. Power Deliv.*, 2011, **26**, (4), pp. 2870–2878

[18] Pramanik, S., Satish, L.: 'Estimation of series capacitance for a three-phase transformer winding from its measured frequency response', *IEEE Trans. Power Deliv.*, 2013, **28**, (4), pp. 2437–2444

[19] Pramanik, S., Satish, L.: 'Time-domain approach to estimate series capacitance of an isolated phase winding of a transformer', *IEEE Trans. Power Deliv.*, 2014, **29**, (4), pp. 1939–1945

[20] Degeneff, R.C.: 'A general method for determining resonances in transformer windings', *IEEE Trans. Power Appar. Syst.*, 1977, **96**, (2), pp. 423–430

[21] Todhunter, I.: '*An elementary treaty on the theory of equations, with a collection of examples*' (Macmillan and Co, London, 3rd edn.)

[22] Guillemin, E.A.: '*Synthesis of passive networks*' (Wiley, New York, 1962)

9 Appendix 1

To verify the existence of a single positive root for (16), two conditions for k are examined:

9.1 Case A: $1 < k < 2N$

In case $k < 2N$, the coefficient of γ^N is always positive. Since k is always greater than 1, the constant term $\beta_0(1-k)$ in (16) is always negative. Since the first term is positive and the last term is negative, following are the conditions for the existence of a single positive root by Descartes' rule-of-signs.

1. There should not be any sign change observable in any of the powers of γ^{N-1} to γ. This is a trivial condition.
2. If there is sign change (from positive to negative) in the coefficients of any power of γ, all the coefficients succeeding it should also be negative. This is examined next.

Theorem 1: If any of the coefficients of (16) become negative, then all the other coefficients succeeding it will also be negative.

Proof: Let c_j be each coefficient of (16). Assume that one of the coefficients of $f(\gamma)$ is negative. Let that coefficient be c_i. We have to prove that $c_j < 0$, $\forall j < i$. The jth coefficient can be represented as

$$
c_j = \beta_j\left(2N\frac{\delta_j}{\beta_j} - k\right) \tag{24}
$$

Since $c_i < 0$

$$\Rightarrow \frac{\delta_i}{\beta_i} < \frac{k}{2N} \tag{25}$$

However, from Tables 2 and 3 it can be observed that for any value of N

$$\frac{\delta_N}{\beta_N} > \frac{\delta_{N-1}}{\beta_{N-1}} > \cdots \frac{\delta_0}{\beta_0} \tag{26}$$

From (25) and (26)

$$\begin{aligned} \frac{\delta_{i-1}}{\beta_{i-1}} &< \frac{k}{2N} \\ \frac{\delta_{i-2}}{\beta_{i-2}} &< \frac{k}{2N} \\ &\vdots \\ \frac{\delta_1}{\beta_1} &< \frac{k}{2N} \end{aligned} \tag{27}$$

From (24) and (27), all the coefficients c_j are negative $\forall j < i$. Hence, the theorem is proved.

Therefore, if the value of Π_{scnf}/Π_{ocnf} lies between 1 and $2N$, there will always be only one positive real root for (16).

9.2 Case B: $k > 2N$

In case $k > 2N$, the first term in (16) becomes negative. The last term is also negative. Hence, there will be NO single positive real root for (16), irrespective of the sign of other coefficients. However, such a situation has not been encountered, neither during simulation nor in any of the practical measurements. Thus, this option can safely be ruled out. □